Supplementary Appendix

Methods

1. Calculation of received dose intensity of ICE chemotherapy

The ICE chemotherapy protocol consisted of ifosfamide (1.5g /m^2), carboplatin (100 mg/m^2), and etoposide (150mg/m^2) on days 1-4 repeated every 4 weeks for 6 cycles (see reference 10; Fiegl et al. 2004).

The patient received the modified ICE regimen as follows: ifosfamide (1.5 g/m^2), carboplatin (100 mg/m^2), and etoposide (150 mg/m^2) on day 1 and day 3 repeated every 3 weeks over 11 cycles. The received dose intensity (DI) was calculated:

37.4 g/m^2 ifosfamide + 2.49 g/m^2 carboplatin +3.74 g/m^2 etoposide.

Total dose (mg)/body surface area x no. of weeks.

DI of ifosfamide = 634.9 mg/m^2/week.

DI of carboplatin = 42.3 mg/m^2/week

DI of etoposide = 63.5 mg/m^2/week

2. Immunohistochemistry of skin biopsy taken after 1st cycle of regional hyperthermia plus low-dose chemotherapy

5 µm standard tissue sections of FFPE tumor samples were stained employing a Ventana Benchmark Ultra autostainer (Ventana Medical Systems, Oro Valley, AZ) following the manufacturer's instructions. A detailed description of antibodies and protocols used in this study is summarized in table 1.

Table 1: Antibodies used for histology

Antibody	Dilution	Detection system	Clone	Species	Manufacturer
CD3	1:150	UltraView	SP7	monoclonal rabbit	Zytomed
CD4	1:500	Optiview	4B12	monoclonal mouse	Leica
CD8	1:50	UltraView	C8/144B	monoclonal mouse	Medac (Cell Marque)
CD56	Ready to use	UltraView	123C3	monoclonal mouse	Ventana
Granzyme B	1:30	UltraView	GrB-7	monoclonal mouse	DakoCytomation

Immunohistochemistry fine needle tumor aspirate (October 2010) before treatment with regional hyperthermia plus low-dose chemotherapy

Immunohistochemistry of the fine needle tumor aspirate was performed on a BenchMark XT automated stainer (Ventana, Tucson, AZ) with antibodies against CD3 (clone MRQ39), CD56 (clone MRQ42), PD-L1 (clone SP263) and Desmin (clone 33) using the ultraVIEW DAB Detection Kit (all reagents from Ventana, Tucson, AZ). Briefly, the tissue sections were deparaffinized with EZ Prep at 75°C and 76°C, heat pretreated in Cell Conditioning 1 (CC1) for antigen retrieval at 76°C – 100°C and then incubated with the primary antibody diluted in antibody diluent after inactivation of the endogenous peroxidase using UV-inhibitor. Antibody binding was detected using DAB as chromogen and counterstained with hematoxylin for 10 min with subsequent bluing in bluing reagent for 10 min. Slides were then dehydrated manually by alcohol washes of increasing concentration (70%, 96%, 100%) and xylene and coverslipped using Pertex® mounting medium (Histolab, Goeteborg, Sweden).

3. Europium Assay

Effector cells: PBMCs isolated by Ficoll density gradient centifugation were washed, counted and resuspended in RPMI 1640 medium supplemented with 10% FCS, in the absence and presence and 100 IU/ml IL-2 (Proleukin, Novartis) at a cell density of 5 x 10^6/ml. The cells were incubated for 4 days at 37°C, 5% CO_2 in a humidified atmosphere. After 2 washing steps, cells were used as effector cells in the Europium assay (Perkin Elmer) at effector to target (E:T) ratios ranging from 10:1 to 0.3:1.

Target cells: K562, a human chronic myelogenous leukemia line, a classical NK target, was maintained in culture in RPMI 1640 medium supplemented with 10% (vol/vol) FCS at constant cell densities of <0.5 x 10^6 cells/ml. Approximately 5 x 10^6 target cells were labeled in 1 ml labeling buffer supplemented with 20 µM Eu $(DH3C00)^{3+}$, 100 µM DPTA and 0.5 mg dextran sulfate for 20 min at room temperature. After stopping the reaction with 30 µl of 100 mM $CaCl_2$ per ml, cells were washed and resuspended in RPMI 1640 medium supplemented 10% FCS at a cell density of 5 x 10^3 cells/100µl.

Labeled target cells were dispensed in 96-well round-bottom well plates together with suspensions of effector cells at equal volumes at E:T ratios ranging from 20:1 to 0.65:1 for 4 h at 37°C in a humidified atmosphere. Then, supernatants (20 µl) were harvested and transferred into another 96 well plate. After addition of 200 µl enhancement solution fluorescence was measured in a time-resolved fluorometer.

4. Multiparameter flow cytometry

PBMCs were isolated using Ficoll density gradient centrifugation and stored frozen in liquid nitrogen until analysis. For flow cytometry, PBMCs were defrosted and stained with antibody cocktails as following:

Analysis of NK cell subsets and NKG2D on NK cells and T cells of PBMCs of the 2nd treatment cycle used anti-CD3-PerCP (BD Pharmingen), anti-CD56-FITC (BD Pharmingen) and anti-NKG2D-PE (R&D Systems). PBMCs of all other treatment cycles used anti-CD3 Pacific Blue (BD Pharmingen), anti-CD56 Alexa Fluor-700 (BD Pharmingen) with anti-NKG2D-APC (R&D Systems), and live/dead fixable blue dead stain kit (Molecular Probes); or CD56-APC (Beckman Coulter) with CD16-Alexa Fluor A700 (Caltag).

Analysis of the T cell differentiation states was performed with antibody cocktail anti-CD3 Pacific Blue (BD Pharmingen), anti-CD8 AmCyan (BD Pharmingen), anti-CD4-

APC-Cy7 (BD Pharmingen), anti-CD45RA-PerCP-Cy5.5 (eBioscience), anti-CCR7-PE (eBioscience), live/dead fixable blue.
Analysis of Treg cells included anti-CD3-Pacific Blue (BD Pharmingen), anti-CD4-APC-Cy7 (BD Pharmingen), anti-CD25-FITC (BD Pharmingen), anti-FOXP3-APC (eBioscience) and live/dead fixable blue. The anti-FOXP3 antibody was added after fixation and permeabilization using the FOXP3 staining buffer (eBioscience). Parallel samples were stained with isotype matched control antibodies. Acquisition was done on a Calibur instrument (BD) (PBMC of the 2^{nd} treatment cycle) or on LSRII (BD) (all other PBMC samples). Analysis was performed using FlowJo (Tree Star). Gates were set according to control isotype staining.

5. Statistics

Statistical analysis was performed to add a quantitative value to the descriptive figures of single measurements at different times over the disease course of one patient or between samples taken from the patient and father at the same time point. To obtain a statistics value for the change in frequency of $CD56^{bright}$ cells (Figure 3B) during the treatment we looked at the measurements before each treatment (square) and after the treatment (circles) separately. We used the null hypothesis for a test, which considers that if the change between subsequent time points is not different, an equal probability for an up or down of the corresponding values would be expected. Formally, a Wilcoxon test was performed to assess the null hypothesis. The following data were observed when subtracting the measurement before each cycle i (i = 2^{nd}, 4^{th}, 5^{th}, 7^{th}, 8^{th}, 9^{th}, 10^{th}) from the measurement before the next documented cycle: 21.35, 1.90, 6.60, 7.40, 10.00, -1.00, 5.90. The p-value of the corresponding Wilcoxon test is 0.03125 indicating that the increase in frequency of $CD56^{bright}$ cells measured before treatment (represented by squares in Figure 3B) is statistically significant.
A similar analysis can be performed for the change in Treg ($CD25^{+}FOXP3^{+}$ within the $CD4^{+}$ T cells) (Figure 3G). The observed differences between consequent measurements are -0.5, -1.3, -0.4, 0.2, -0.9, -1.0, -0.4. Applying the Wilcoxon test based on the same arguments as above, the respective p-value is 0.03125.

Supplementary Figures:

Supplementary Figure S1

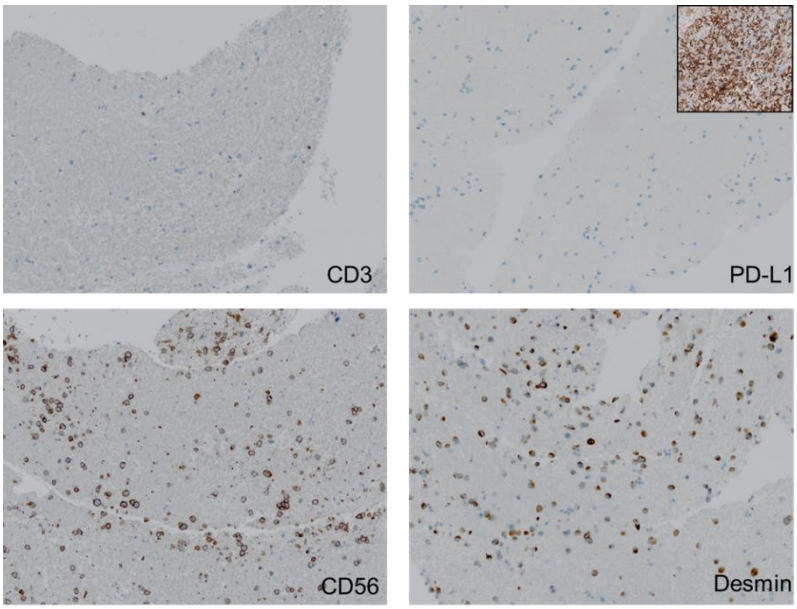

Supplementary Figure S1: Immunohistochemistry of fine needle tumor aspirate taken before treatment with regional hyperthermia plus low-dose chemotherapy. The specimen was taken at the time of relapse after h-SCT. Depicted are: staining with anti-CD3, anti-PD-L1 (insert shows positive control staining), anti-CD56, anti-desmin. Pictures are taken at 200-fold magnification. Desmin-positive cells correspond to tumor cells, anti-CD56 detects aberrant expression on tumor cells. Anti-CD3 reveals very scarce lymphocyte infiltration. There is no positivity of PD-L1, neither on lymphocytes nor on tumor cells.

Supplementary Figure S2:

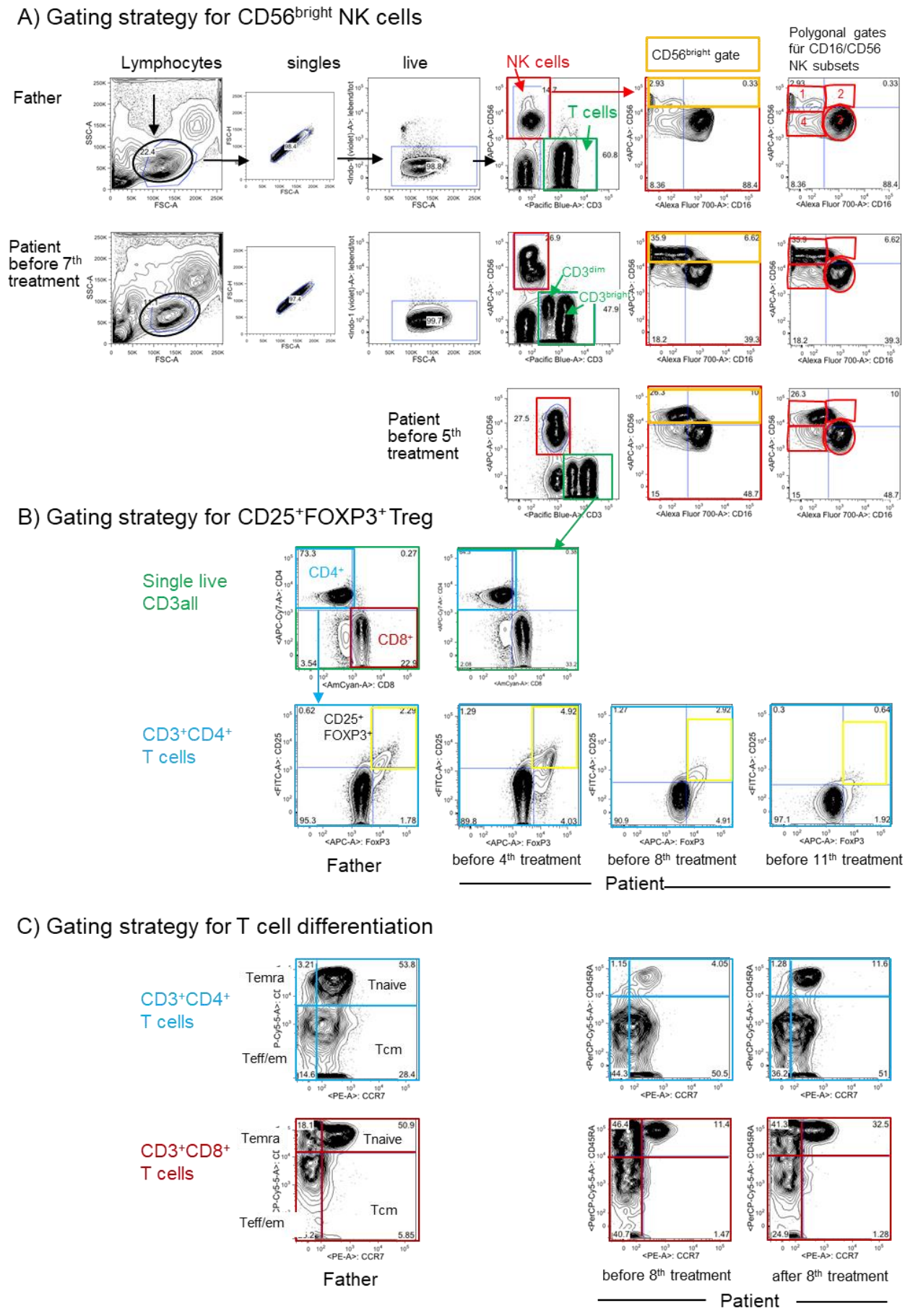

Supplementary Figure S2: Gating strategy

A) Frequency of CD56^{bright} NK cells

Lymphocytes were selected based on FSC/SSC characteristics (left dot plot). Then, duplets were excluded (FSC-A/FSC-H) followed by gating on the live cells (indo-1 violet negative events). Subsequently, NK and T cells were discriminated based on CD56 and CD3 expression (NK cells: CD3^{-}CD56^{+}, red box; T cells: CD3^{+}CD56$^{\pm}$, green box). The frequency of the CD56^{bright} NK cell subset within the NK cells (red box) was determined as the sum of the upper left and upper right quadrants (dark yellow box) in the gated NK cell population. For NK subset specification according to CD56 and CD16 expression intensities, 4 polygonal gates were used (1: CD56^{bright}CD16^{-}; 2: CD56^{bright}CD16^{+}; 3: CD56^{dim}CD16^{+}; 4: CD56^{dim}CD16^{-}). Shown are PBMC of the father (healthy control) and two patient samples, taken after the 5th and 7th treatment cycle. In the patient samples, the CD3^{+} T cell population is clearly subdivided into one population that shows regular CD3 intensity, comparable to the father), and a second population with reduced CD3 intensity (CD3^{dim}).

B) Frequency of CD25^{+}FOXP3^{+} Treg cells

Selected CD3^{+} T cells (see A) were subdivided into CD4^{+} (blue box) and CD8^{+} (brown box) T cells. Among the CD4^{+} T cells, the percentage of those co-expressing CD25 and FOXP3 was identified (upper right quadrant, yellow box). Examples are shown for the father (healthy control) and three patient samples harvested before 4th, 8th and 11th treatment cycle documenting the continuous decline in frequency of CD25^{+}FOXP3^{+} Treg cells.

C) Differentiation state of CD4^{+} and CD8^{+} T cells

Selected CD3^{+} T cells were subdivided for CD4^{+} and CD8^{+} T cells (see A) and B), which were then subcategorized according to the markers CD45RA and CCR7 in naïve (CD45RA^{+}CCR7^{+}, upper right quadrant), effector/memory (Teff/em, CD45RA^{-} CCR7^{-}, lower left quadrant), central memory (Tcm, CD45RA^{-}CCR7^{+}, lower right quadrant) and terminally differentiated T cells (Temra, CD45RA^{+}CCR7^{-}, upper left quadrant). Examples are shown for PBMC of the father (healthy control) and two patient samples (before and after 8th treatment cycle) documenting the patient's low percentages of CD4^{+} Tnaive cells (upper right quadrant) compared to the father (blue arrows) with concomitant strongly enriched Teff/em and Tcm in the CD4^{+} T cells (both lower quadrants); and among the CD8^{+} T cells, the highly enriched Temra populations (upper left quadrant, brown arrow).

Supplementary Figure 3:

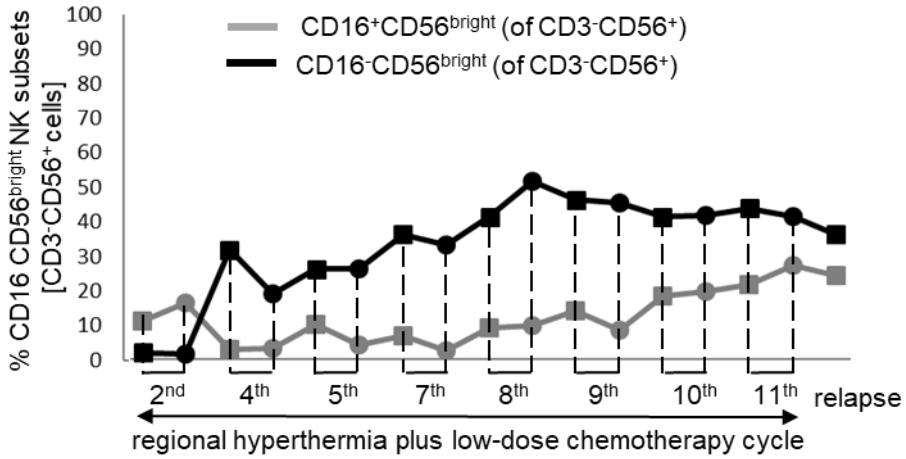

Frequencies of $CD56^{bright}CD16^{+}$ and $CD56^{bright}CD16^{-}$ NK cell subsets during disease course

Shown is the change in frequencies of $CD3^{-}CD56^{bright}$ NK cells specified into $CD16^{+}$ and $CD16^{-}$ subsets in the patient`s PBMCs before (closed squares) and after (closed circles) the 2^{nd}, 4^{th}, 5^{th}, 7^{th}, 8^{th}, 9^{th}, 10^{th}, 11^{th}, treatment cycles and at relapse (4^{th} November 2011). The values are the percentages of all $CD56^{bright}$ NK cells within the NK cell population. The values are derived from polygonal gates 1 and 2 of $CD3^{-}CD56^{+}$ lymphocytes, as shown in Supplementary Figure 2A.